# Growth of Devitrite, $Na_2Ca_3Si_6O_{16}$, in Soda–Lime–Silica Glass

Kevin M. Knowles* and Robert P. Thompson

Department of Materials Science and Metallurgy, University of Cambridge,
27 Charles Babbage Road, Cambridge, CB3 0FS, U.K.

**Abstract**

The morphology and crystal growth of devitrite crystals nucleated heterogeneously on glass surfaces have been studied. The crystals grow as fans of needles, with each needle having a characteristic [100] growth direction with respect to the centrosymmetric triclinic unit cell. An analysis of crystal growth data reported here and a reappraisal of crystal growth data reported in prior studies suggests a best estimate of 260 kJ $mol^{-1}$ for the activation enthalpy for the crystal growth of devitrite along [100], higher than the values previously reported.

*Corresponding author. Email: kmk10@cam.ac.uk

## I. Introduction

The term ‘devitrification’ is used in glass technology to describe the process of crystallization, after which the triclinic crystalline phase, devitrite, $Na_2Ca_3Si_6O_{16}$, is named.[1] This *dreier* quadruple-chain silicate[2,3] is the principal devitrification product in commercial soda–lime–silica glasses.[1,4,5] Literature values for the activation enthalpy for crystal growth for devitrite are given as 135 kJ mol$^{-1}$ and ≈ 220 kJ mol$^{-1}$,[6,7] both based on an analysis of crystal growth data using an Arrhenius plot. The justification for such an analysis given by Deubener *et al.*[7] is that, at large undercooling temperatures below the maxima of growth rates, such a plot of the natural logarithm of the linear crystal growth rate, $u$, against the reciprocal of the absolute temperature, $T$, should yield a straight line with a slope proportional to the activation enthalpy for crystal growth, $Q$, i.e. the activation energy for diffusion governing the rate of transport across the crystal–liquid (or crystal–glass) interface. These two analyses of crystal growth data for devitrite, based on an approximation to the normal model of crystal growth,[8,9] contrast with earlier, empirical, approaches used by Preston[10] and Swift.[11] Preston and Swift were both able to obtain good fits for their crystal growth data for devitrite in terms of the product of the amount of undercooling below the liquidus temperature and the reciprocal of the experimental viscosity of the glass at the temperature under investigation, multiplied by a suitable constant.

In view of the clear discrepancy between the two literature values for the activation enthalpy for crystal growth, and also in view of the two different approaches used to analyse crystal growth data for devitrite, it is perhaps surprising that there has not been a reappraisal of the crystal growth data for devitrite present in the literature. Furthermore, little attention has been given to the specifics of the growth characteristics of devitrite in the literature, other than a recognition that the crystals grow in fans of optically biaxial needles,[4,12–15] and that there is clearly a preferred direction of growth along the axis of the needles. In this article, we report morphological observations of devitrite and crystal growth data on devitrite from a commercial soda–lime–silica glass between 680°C and its liquidus temperature, 965°C. An analysis of our own crystal growth data and a reanalysis of the prior data in the literature suggest that a best estimate for the activation energy for the crystal growth for devitrite is 260 kJ mol$^{-1}$, slightly higher than the estimate of Deubener *et al.*,[7] and significantly higher than the value reported by Zanotto.[6] A very brief summary of some aspects of this work has been reported recently elsewhere in a paper overviewing our recent work on devitrite.[16]

## II. Experimental Procedure

10 mm thick blocks of soda–lime–silica float glass cut into sections 50 mm long and 7 mm wide were obtained from a commercial glass supplier in Cambridge, U.K., Go Glass, as in a previous transmission electron microscope study on devitrite.[17] These blocks were placed in alumina or mullite crucibles for heat treatment in the temperature range 680–970°C for times between 1 and 68 h, either as whole blocks, or cut into smaller blocks, depending on the time and temperature used for heat treatment.

For each heat treatment samples were placed into preheated furnaces. In the initial experiments in the temperature range 680–750°C, it was entirely random which side of the float glass blocks was in direct contact with the crucible material. In later experiments in the temperature range 900–965°C when it had became apparent that, as expected, the as-received top and bottom surfaces of the blocks of float glass which had not been cut mechanically (i.e. the tin bath side of the glass and the side opposite the tin bath side) were clearly less preferred nucleation sites, these two surfaces were chosen to be the sides of the blocks adjacent to the side chosen to be in direct contact with the crucible material. Only the bottom side of the samples were put in direct contact with the crucible material, but during heat treatment at and above 850°C the samples were able to slump sufficiently during heat treatment to contact the sides of the crucible.

After heat treatment, the devitrified blocks were cooled in the furnace for a long enough time to enable them to be taken out of the furnace without causing thermal shock. In practice, 6 hr or more was allowed for the samples to cool down to 200°C or below. For the crystal growth experiments, the critical time was the time immediately after the end of the heat treatment, because additional growth of crystals could occur during this initial cooling period. The temperatures for which the possibility of such additional growth is most relevant were the three temperatures of 900, 925 and 950 °C. Hence, in experiments where crystal growth was examined at these temperatures for periods of 1, 2 and 4 h and in experiments to determine the liquidus temperature for devitrite crystal growth, the furnace door was deliberately opened after heat treatment to induce air cooling of the samples down to 600°C, and therefore to all intents and purposes cause cessation of crystal growth after the period of heat treatment.

Despite some cracking of the samples because of the differential thermal contraction between the devitrified glass blocks and the crucibles, there were sufficiently large crack-free regions in the heat-treated blocks for samples to be analysed by standard ceramographic

procedures for both polarized light transmitted light optical microscopy and scanning electron microscopy. The polarized light microscopy was undertaken on a XPL-3230 polarization microscope manufactured by Guangdong Silique International. Scanning electron microscopy was performed at 15 kV on a JEOL 5800LV machine.

In determining crystal growth rates for each temperature from microscopical observations, a search was made for the longest crystals that could be found in samples as a function of heat treatment, irrespective of where they had nucleated. In practice, the longest crystals were found on the sides of the blocks which had been cut mechanically – the high finish float glass faces showed the least number of nucleation events and the freshly cut and contaminated surfaces showing much higher numbers of nucleation events. This was all consistent with classical nucleation and growth theory, i.e. crystals nucleated on heterogeneities on the surfaces of the blocks, after which growth of crystals occurred both parallel to the surface and also into the bulk interior of the glass.

Needle lengths were measured on the surfaces of samples and/or in cross-sections parallel to the original 50 mm length of the blocks. No evidence was found for growth along the surface of the glass being any different from growth into the bulk. In places where spherulites were not impinging on each other, near-perfect hemispheres were seen growing from nucleation sites, with the maximum needle length being found both parallel to the surface and perpendicular to the surface in samples. The assessment of the length of the longest needles found in a heat-treated sample was often compromised by clear overlapping of crystals in fans of needles. Hence, anomalously long lengths of needles could be judged not to be true lengths of a single needle, but rather separate needles seen in projection arising from separate nucleation events, giving the appearance of long needles. Repeated measurements were undertaken so that thousands of needles in spherulites were examined per sample. Lengths were recorded of a representative number of what were judged to be the longest needles per sample.

The chemical composition of the samples of float glass used for the experiments was determined using electron probe microanalysis on a Cameca SX-100 operating at a voltage of 15 kV and a beam current of 20 nA with a 10 μm beam size. The sensitivity of this instrument allowed confirmation that the samples had a tin-rich side: clear evidence for tin could be found from point analyses within 30 μm of the edge of one of the high finish float glass faces, but not the other. The chemical composition established for the float glass from

the average of eight point analyses on one particular sample, with each analysis lasting 4.5 minutes, is shown in Table 1.

## III. Experimental Results

As a result of the heat treatment of commercial float glass below the devitrite liquidus temperature, devitrite crystals nucleate heterogeneously on the surfaces of the float glass. Subsequent growth of these crystals is then parallel to the surface and also into the bulk of the glass. It is evident that the devitrite crystals are produced in characteristic fans of needles, as can be seen in the polarized light micrograph in Fig. 1, taken with a sensitive tint at 45° to the polarizer (vertical direction) and analyser (horizontal direction). The micrograph is taken from a slice sectioned out of the heat-treated glass block and prepared as a thin section using standard mineralogical specimen preparation procedures for thin sections. It was evident from crystal growth measurements that the fans of needles in Fig. 1 were nucleated some time after the start of the heat treatment of 17 h at 850°C had begun, because spherulites with significantly longer needles than those seen in Fig. 1 were readily apparent elsewhere in this sample.

The crystals in Fig. 1 are the same as the optically biaxial crystals first described by Insley[12] and later described by Morey and Bowen[4] as the compound '$Na_2O$,3CaO,6$SiO_2$' having an elongation along 'γ' with refractive indices $n_\gamma$ = 1.579, $n_\alpha$ = 1.564 and an optic axial angle of about 75°, therefore implying that $n_\beta \approx 1.570$, in good agreement with optical properties for this phase reported later by Peck.[13] They are also identical to the devitrite crystals found by Holland and Preston[14,15] in their 1930s studies on the identification of crystalline products found in commercial glasses and those grown by Swift for his 1940s work.[11,18] They are readily distinguishable from other devitrification products possible in commercial float glass such as cristobalite and wollastonite. Cristobalite has negative relief relative to the surrounding glass, for which it can be assumed that the refractive index is 1.52, following Hrma *et al*.,[5] and it occurs as small spherulites with characteristic internal twinning arising from the $\beta \rightarrow \alpha$ cristobalite phase transition which occurs on cooling down to room temperature from a temperature above 275°C.[19] Wollastonite has a noticeably higher positive relief relative to the surrounding glass than devitrite because of its higher principal refractive indices, quoted by Insley[12] as $n_\alpha$ = 1.616, $n_\beta \approx 1.629$ and $n_\gamma$ = 1.631, and it occurs as crystals

described by Hrma *et al*. as columnar and bladed.[5] Also, unlike devitrite, it has a variable sign of elongation because the β direction is parallel to the elongation.[12]

Both Morey and Bowen[4] and Peck[13] surmised that devitrite was orthorhombic because of an extinction direction parallel to the needle axis, and observations of crystals with four-, six- or eight-sided prisms,[13] although Peck[4] only noted diamond shaped cross-sections of needles. More recent studies using X-ray diffraction have determined that devitrite actually has a triclinic unit cell.[2,3,20] With respect to the centrosymmetric $Z = 2$ triclinic unit cell for devitrite described recently by Kahlenberg *et al*.[3] with lattice parameters $a = 7.2291$ Å, $b = 10.1728$ Å, $c = 10.6727$ Å, $\alpha = 95.669°$, $\beta = 109.792°$ and $\gamma = 99.156°$, the elongation is along [100]. This is consistent with Fig. 1 because needles in this micrograph aligned either with the polarizer or the analyzer take the colour of the sensitive tint. A further feature of the unit cell is that the interplanar spacings of the (010) and (001) planes are almost identical (to within 0.1 pm);[17] it is evident from Fig. 3 of Knowles and Ramsey[17] of the cross-section of a devitrite needle seen along [100] that the four-sided prisms reported by Morey and Bowen and Peck will be bounded by {010} and {001) planes, while the eight-sided prisms are bounded by {010}, {001}, {011} and $\{ 01\bar{1} \}$ planes. The angle between (010) and (001) is 80.54°; omission of either the {011} or the $\{ 01\bar{1} \}$ planes will produce six-sided prisms with cross-sections which will be six-sided in cross-section, and therefore hexagonal, although evidently not the shape of a regular hexagon.

Detailed observations of the fans of needles over the various heat treatment schedules suggested that nucleation of devitrite did not occur heterogeneously within the bulk glass, nor did it seem to occur readily on the side of pre-existing needles. Instead, strong evidence was found for small-angle branching within fans to enable the needles of devitrite to fill three-dimensional space in the form of spherulites.[21] An example of small-angle branching seen in transmitted polarized light microscopy is shown in Fig. 2.

Linear crystal growth rates parallel to [100] were determined by measuring the length of the longest individual needles that could be seen in thin sections after heat treatment. Attention was focused on both relatively low temperature heat treatments of 680 – 750°C, where growth was relatively slow and heat treatment times long, and relatively high heat treatments of 900–970°C (Table 2), i.e. a low temperature regime at large undercooling temperatures and a temperature regime in which there is relatively modest undercooling and a maximum in the crystal growth rate. In determining crystal growth rates, it was assumed that nucleation of the longest needles happened at the start of each heat treatment. At the lower

heat treatment temperatures this is a realistic assumption because the critical sizes for nucleation will be small, and numerous observations were made with long heat treatment times to establish that crystal growth was indeed linear within experimental error in this temperature regime. Crystal growth data from the 900°C and 925°C heat treatments as a function of time are shown in Table 3, from which it is readily apparent that the crystal growth is also linear with time within experimental error. Unfortunately, it is difficult to establish absolute error limits reliably in such crystal growth data. Thus, for example, for needles seen in thin sections, it is possible that needle length is somewhat underestimated because the needles selected for measurement are not necessarily perpendicular to the beam of light. At 950°C there were noticeably fewer nucleation events, and the length of one anomalously long needle after the 4 h heat treatment was taken to be an unreliable indicator of the true crystal growth rate because it seemed not to be a true single needle. Hence, at 950°C it is entirely possible that the growth rate shown in Table 1 is a lower bound estimate of the true crystal growth rate.

Extended heat treatments between 18 h and 24 h at 960, 965 and 970°C followed by air cooling to 600°C to avoid any unintended crystal growth during cooling showed clear evidence for devitrite growth at 960°C, a few isolated examples of devitrite growth at 965°C and no evidence of devitrite growth at 970°C. In all of these three heat treatments wollastonite was the dominant devitrification product, forming as characteristic bladed crystals, such as in the examples shown in Fig. 6 of Hrma *et al*.[5] The estimated liquidus temperature for devitrite in the float glass examined in this study is therefore just above 965°C, in good agreement with the quoted liquidus temperature for devitrite of 965 ± 1.6°C obtained from the study of a number of float glass compositions in the commercial float glass composition region studied by Hrma *et al*.[5] The relative insensitivity of the liquidus temperature for devitrite to composition within the commercial float glass composition region was noted by Hrma *et al*.[5]

The data in Table 1 are consistent with the crystal growth data for devitrite obtained by Swift in the temperature range 750°C – $T_{liq}$ for a soda–lime–silica glass with 2 wt% $Al_2O_3$ with a liquidus temperature, $T_{liq}$, of just over 1000°C,[18] and with crystal growth data for devitrite obtained by Swift in soda–lime–silica glasses containing magnesia and alumina.[11] In this context, it is relevant that the addition of small amounts of magnesia to soda–lime–silica silica glasses has two effects: (i) a lowering of the liquidus temperature for devitrite, and (ii) a

lowering of the rate of crystal growth of devitrite. Our crystal growth data for devitrite are also consistent with the results from Deubener *et al*.[7] and Dietzel and Flörke.[22]

There is, however, a difference between our data at low temperatures and the data in Fig. 4 of Zanotto[4]: for example, our data shows a growth rate of 5.2 μm $h^{-1}$ at 750°C, whereas it is apparent from Fig. 4 of Zanotto[6] that the quoted growth rate at this temperature is noticeably lower: 0.8 μm $h^{-1}$. It is possible that there is a systematic factor of 6–7 or so here which might explain this discrepancy, since our own analysis of Zanotto's data in Section IV shows that the data in Fig. 4 of his paper at 750°C, 775°C and 800°C is internally self-consistent.

## IV. Data analysis

### *(1) Crystal Growth Modelling*

For undercooled one-component liquids, the linear crystal growth rate can be written in the form[8]

$$u = a_0 \nu \exp\left(-\frac{Q}{RT}\right)\left[1-\exp\left(-\frac{\Delta g}{RT}\right)\right] \qquad (1)$$

where $u$ is the growth rate, $a_0$ is a molecular diameter (or jump distance), $\nu$ is a vibration frequency taken to be independent of temperature, $T$ is the temperature (in K), $R$ is the gas constant, $Q$ is the activation energy for diffusion governing the rate of transport of material across the crystal–liquid interface and $\Delta g$ is the free energy change $mol^{-1}$ in transforming from the liquid to the solid. This model, known as the normal or continuous growth model,[9] is based on the assumption that the heat of crystallisation is dissipated sufficiently rapidly that the temperature at the crystal–liquid interface can be assumed to be constant. A modification of this model is the screw dislocation model, in which the interface is regarded as smooth, but imperfect, on the atomic scale, with growth taking place at steps generated by screw dislocations intersecting the growing interface.[9]

Notwithstanding the fact that the stability field in the $Na_2O$–CaO–$SiO_2$ phase diagram of devitrite is relatively far from its own chemical composition of 10.5 wt% $Na_2O$, 28.5 wt% $Na_2O$ and 61 wt% $SiO_2$,[4,23] it is clearly tempting to model the crystal growth of devitrite in float glass in terms of an equation similar in form to Eq. (1). Indeed, prior to the development of the normal growth model, Preston[10] asserted that the early stages of crystallisation in a soda–lime–magnesia–silica glass could be represented by an equation of the form

$$u = C\left(T_{\mathrm{liq}} - T\right)\exp\left(-\frac{Q}{RT}\right) \tag{2}$$

with $C$ a temperature-independent constant and $T_{\mathrm{liq}}$ being the liquidus temperature for devitrite, i.e. the maximum temperature at which devitrite is in equilibrium with the soda–lime–magnesia–silica glass. It is notable in the context of the analysis here that the glass analysed by Preston was of a chemical composition similar to contemporary float glass. Preston assumed in his analysis that the viscosity of glass could be represented by an Arrhenius form with what can be identified as an activation free energy $Q$ for viscous flow, arguing that departures from the Arrhenius form are likely to be less than observed variation in crystal size and growth.

If the entropy difference, $\Delta s$, between the crystal and the liquid (or glass) is sensibly temperature-independent in the temperature range of interest, the substitution

$$\Delta g = \Delta s\left(T_{\mathrm{liq}} - T\right) \tag{3}$$

can be made in Eq. (1).[8,9] For sufficiently small $\Delta g$, it is evident that Eq. (1) takes the form of Eq. (2) with $C = a_0 \nu \Delta s / R$.

An alternative interpretation of Eq. 1 is to replace the term

$$a_0 \nu \exp\left(-\frac{Q}{RT}\right) \tag{4}$$

by

$$\frac{k_{\mathrm{B}} T}{3\pi a_0^2 \eta} \tag{5}$$

using the Stokes–Einstein relationship, where $k_{\mathrm{B}}$ is Boltzmann's constant and $\eta$ is the shear viscosity of the glass.[9] For sufficiently small $\Delta g$, this leads naturally to the type of equation envisaged by Preston and the specific equation considered by Swift.[11]

Recent consideration of the relevance of using the Stokes–Einstein relationship for 'fragile' liquids and multicomponent systems has called into question the description of diffusion in terms of viscosity, implying that instead the actual diffusion coefficient controlling crystal growth is better expressed as an effective diffusion coefficient arising from a combination of the diffusion coefficients of all the components of the system under consideration.[24,25] This sentiment is in accord with a recent study of the devitrification of

Borofloat 8330 glass in which the value of $Q$ determined for the growth of cristobalite from the sodium borosilicate glass (175 – 195 kJ mol$^{-1}$) was significantly lower than the effective Arrhenius activation energy for viscous flow of > 300 kJ mol$^{-1}$ over the temperature range of 660 – 850°C examined.[26]

As many authors have noted, the viscosity–temperature dependence for many glass-forming systems can be modelled using the Vogel–Fulcher–Tammann–Hesse (VFTH) equation,[27]

$$\log_{10} \eta = A + \frac{B}{T - T_0} \tag{6}$$

for constants $A$, $B$ and $T_0$. Furthermore, knowledge of the chemical composition of a silicate glass can be used to establish the appropriate $A$, $B$ and $T_0$ for that glass. Given the chemical composition of the float glass in Table 1, estimates of $A$, $B$ and $T_0$ from the models of Lakatos *et al.*[28], Fluegel *et al.*[29] and Fluegel[30] are shown in Table 4. The estimates from the Fluegel *et al.*[29] model were described as 'outside optimal composition/interaction limits' for which viscosity estimations are still expected to be accurate to ± 12°C.

Despite the estimates from the Fluegel *et al.*[29] model being outside the optimal composition/interaction limits, it is apparent that all three models predict very similar values of $A$, $B$ and $T_0$ for the glass in Table 1 so that graphs of viscosity–temperature plots will be very similar. Consideration of Eq. (6) between 680°C (953 K) and 965°C (1238 K), the liquidus temperature, for the Fluegel[30] model for all the eight oxide compositions in Table 1 shows that, while a plot of ln η against 1/$T$ (with $T$ in K) is clearly not a straight line, quite a reasonable linear fit can be nevertheless be obtained throughout this temperature range (Fig. 3). Within this entire temperature range, this linear fit predicts an apparent activation energy of 323 kJ mol$^{-1}$.

In general, if we force a straight line fit between two temperatures $T_1$ and $T_2$ within this range at which the viscosities are $\eta_1$ and $\eta_2$ respectively, the apparent Arrhenius activation energy, $Q$, for a viscosity–temperature dependence of the form $\eta = \eta_0 \exp(Q/RT)$ for a constant $\eta_0$ is given by

$$\frac{Q}{R} = \frac{\ln \eta_1 - \ln \eta_2}{\frac{1}{T_1} - \frac{1}{T_2}} = B \ln 10 \frac{T_1 T_2}{(T_1 - T_0)(T_2 - T_0)} = \frac{B \ln 10}{\left(1 - \frac{T_0}{T_1}\right)\left(1 - \frac{T_0}{T_2}\right)} \tag{7}$$

using Eq. (6). Hence, as $(T_1 - T_2) \rightarrow 0$,

$$\frac{Q}{R} = \frac{\mathrm{d}(\ln \eta)}{\mathrm{d}(1/T)} = \ln 10 \frac{\mathrm{d}(\log_{10} \eta)}{\mathrm{d}(1/T)} = \frac{B \ln 10}{\left(1 - \frac{T_0}{T}\right)^2} \tag{8}$$

i.e., in words, the apparent Arrhenius activation energy $Q$ decreases as the temperature increases (i.e. as $1/T$ decreases) within the temperature range of interest below the liquidus.

For the data in Fig. 3, the lower limit on $Q$ is therefore attained at 965°C: for $B$ = 4514.54 K and $T_0$ = 246.949°C, this is 257 kJ mol$^{-1}$, still noticeably higher than the literature values of 135 kJ mol$^{-1}$ and ≈ 220 kJ mol$^{-1}$ quoted for crystal growth of devitrite.[6,7]. Thus, on the basis of this calculation, it would seem reasonable to conclude from a comparison with the literature values of 135 kJ mol$^{-1}$ and ≈ 220 kJ mol$^{-1}$ that the actual diffusion coefficient controlling crystal growth of devitrite in soda–lime–silica glass is not determined by the viscosity of the soda–lime–silica glass.

If instead of comparing crystal growth rates with viscosity–temperature dependence, we retain the form of Eq. 1 for a reasonable representation of the crystal growth rate of devitrite in soda–lime–silica glass, then, using Eq. 3, we can recast Eq. 1 in the form

$$\ln\left(\frac{u}{\Sigma}\right) = \ln A_0 - \frac{Q}{RT} \tag{9}$$

where $A_0 = a_0 \nu$ and $\Sigma$ is defined by the equation

$$\Sigma = \left[1 - \exp\left(-\Delta s_\mathrm{r}\left(\frac{1}{T_\mathrm{r}} - 1\right)\right)\right] \tag{10}$$

where $T_\mathrm{r} = T/T_\mathrm{liq}$ is the reduced temperature (with $T$ and $T_\mathrm{liq}$ in K) and $\Delta s_\mathrm{r} = \Delta s/R$ is the reduced melting entropy.[26]

We now associate $Q$ with the (unknown) rate-determining step in terms of transport across the liquid–crystal interface. For example, this could actually be the transport of atoms in float glass away from the volume of material transforming into devitrite because of the known chemical composition difference between float glass and devitrite.

It is apparent from Eq. (10) that if

$$\Delta s_\mathrm{r}\left(\frac{1}{T_\mathrm{r}} - 1\right) \to \infty \tag{11}$$

Eq. (9) reduces to an analysis of the crystal growth data in terms of an Arrhenius plot so that $u$ is of the form

$$u = A_0 \exp\left(-\frac{Q}{RT}\right) \tag{12}$$

i.e. under these circumstances, Eq. (9) reduces to the very approximation used in the analyses of both Zanotto[6] and Deubener *et al.*[7] It is evident that such analyses can only be justified, even approximately, at large undercooling temperatures and/or large values of $\Delta s_r$. More significantly, the analysis of Moğulkoç *et al.*[26] shows that the use of Eq. 11 will necessarily give a lower bound to $Q$.

It is evident that we can use Eq. 9 to analyse the crystal growth of devitrite treating $\Delta s_r$ as a variable, just as Moğulkoç *et al.*[26] did for their analysis of the growth of cristobalite in Borofloat 8330 glass. As $\Delta s_r$ approaches 0, it can be seen from equation (10) that $\Sigma$ approximates to

$$\Sigma = \Delta s_r\left(\frac{1}{T_r} - 1\right) \tag{13}$$

and so, under these circumstances, to examine what might be expected at a lower limit of $\Delta s_r = 0$, it is appropriate to plot a graph of $\ln\left(uT_r/(1-T_r)\right)$ against $1/T$ to expect to produce a straight line, rather than plotting $\ln\left(u/\Sigma\right)$ against $1/T$ to expect to produce a straight line.

The results of such an analysis of the data in Table 2 are shown in Fig. 4 for a liquidus temperature of 965°C (1238 K) and for $\Delta s_r$ values of 0, 5, 14, 50 and ∞. To force reasonable straight line fits for the $\Delta s_r$ values of 50 and ∞, the data points at 925°C and 950°C have had to be disregarded.

It is apparent that each of the best fit lines for the various $\Delta s_r$ values chosen has a linear correlation coefficient very close to 1, so that unless a particular value of $\Delta s_r$ is identified as being a best estimate of the 'correct' $\Delta s_r$, it is not possible to determine on the basis of best fit which line is preferable. Furthermore, it is apparent from the gradients of each line that, as expected from the analysis of Moğulkoç et al.,[26] the value of $Q$ determined from Eq. (9) decreases as $\Delta s_r$ increases, so that a lower bound on $Q$ of 244 kJ mol$^{-1}$ is obtained when $\Delta s_r = \infty$, and an upper bound on $Q$ of 311 kJ mol$^{-1}$ is obtained when $\Delta s_r = 0$.

Fortunately, there are experimental measurements from which a value of $\Delta s_r$ can be determined. Kröger and Kreitlow[31] quote a value in kcal mol$^{-1}$ for the heat of devitrification of devitrite equivalent to –143.6 kJ mol$^{-1}$ (Table 5 of [31]). For a liquidus temperature of 965°C (1238 K), the corresponding value of $\Delta s_r$ is 14, for which $Q$ is estimated to be 262 kJ mol$^{-1}$ from Fig. 4. This value of $\Delta s_r$ is high relative to other silicate glasses,[9] but it must be recognised that a formula unit of devitrite comprises 27 ions, and is therefore a relatively complex entity. Fokin *et al*.[9] argue that such high a value of $\Delta s_r$ make the screw dislocation growth model more plausible than the normal growth model for crystal growth; however, for the purposes of our analysis here, all this introduces is a dimensionless term $f$ (< 1) to multiply $A_0$ in equation (9) to specify the fraction of sites where atoms can be added or removed preferentially during crystal growth.

A plot of crystal growth rate against temperature for the data in Table 1 is shown in Fig. 5 and compared with Eq. (9) with $Q$ taking a value of 262 kJ mol$^{-1}$, a $\Delta s_r$ of 14, a $T_{liq}$ of 1238 K, and an $A_0$ of $1.8 \times 10^{14}$ μm h$^{-1}$, corresponding to $4.72 \times 10^4$ m s$^{-1}$. For sensible values of a jump distance, taken to be of the order of ≈ 3.6 Å for one formula unit of $Na_2Ca_3Si_6O_{16}$ growing along [100], this implies a relatively high value of ν of $1.3 \times 10^{14}$ s$^{-1}$, but one which is certainly plausible.

### *(2) Reanalysis of other devitrite crystal growth data*

The methodology established in the previous sub-section can be used to reanalyse the crystal growth data for devitrite available in the literature. The data from Fig. 5 of Swift,[18] also shown in Fig. 8.19b of Kingery, Bowen and Uhlmann,[32] is analysed in Fig. 6 in the same way that we have analysed our own experimental data. For a liquidus temperature of 1006°C, measured on Fig. 5 of Swift,[18] and a $\Delta s_r$ of 14, $Q$ is estimated to be 255 kJ mol$^{-1}$. Once again, to present the growth data with reasonable straight line fits, the data for the $\Delta s_r$ value of ∞ has had to be selectively edited so that the growth data for 975°C and 1000°C is not used.

Analyses of the data from curve I in Fig. 4 of Dietzel and Flörke,[22] the data for the bulk glass surface in Fig. 10a of Deubener et al.[7] and Fig. 4 of Zanotto[6] are shown in Figs. 7–9 respectively. The liquidus temperature for the glass examined by Dietzel and Flörke was taken from Fig. 4 of their work to be 962°C. For a $\Delta s_r$ of 14, $Q$ is estimated to be 277 kJ mol$^{-1}$ using their growth data. As before, for higher values of $\Delta s_r$ of 50 and ∞, the

data has had to be selectively edited so that the growth data at the higher growth temperatures of 925°C and 950°C are not used to produce Fig. 7.

In the graphs analysing the crystal growth data from Deubener *et al.*[7] shown in Fig. 8, a liquidus temperature of 930°C has been assumed. This is a significantly lower liquidus temperature than for our own samples of float glass, but in their data in Fig. 10a of their paper, the peak in crystal growth occurs between 883°C and 890°C for devitrite crystals grown on the bulk glass surface, and the continuation of the line they have drawn through their data points suggests this temperature for the liquidus temperature for devitrite. Were a higher liquidus temperature to be used, such as 940°C through a simple linear extrapolation of the line they have drawn in Fig. 10a, the data fits the trendlines in Fig. 8 noticeably less well, significantly lowering the squares of their linear correlation coefficient to < 0.9. For the data for $\Delta s_r = 50$, we have only used growth data in the temperature range 840 – 890°C; for the data for $\Delta s_r = \infty$, we have used only those four data points between 840°C and 868°C that Deubener *et al*. themselves used when plotting their Fig. 14a, from which they extracted a $Q$ of 216 kJ mol$^{-1}$.

Our own analysis of the data for $\Delta s_r = \infty$ in Fig. 8 gives a $Q$ of 220 kJ mol$^{-1}$, agreeing very well with Deubener *et al.*'s analysis. For $\Delta s_r = 14$, the predicted $Q$ increases to 246 kJ mol$^{-1}$, while if we had assumed $\Delta s_r = 0$, $Q$ would be predicted to be 310 kJ mol$^{-1}$.

Zanotto's data in Fig. 4 of his paper suggests growth rates for the diameter of devitrite crystals of 0.8, 1.16 and 1.74 μm h$^{-1}$ at 750, 775 and 800°C respectively.[6] These growth rates are significantly slower than growth rates measured by others at these temperatures and contrast with the growth rates reported by Dietzel and Flörke, who show a growth rate for devitrite of 2.9 μm min$^{-1}$ at 800°C in the glasses they examined. It is entirely possible, as Deubener et al.[7] argue, that relatively small changes of glass composition can account for these differences, as can factors of two arising from whether diameters of crystals are being measured or length of needles, but since Zanotto's observations were on what is also described as float glass,[6] the possibility arises that there is a systematic measurement error which might account for this marked difference between his rates of crystal growth and our data in Table 1.

It is evident from Fig. 9 that the data from Fig. 4 of Zanotto is internally self-consistent. Our reassessment of his data show that for $\Delta s_r = \infty$, i.e. for an Arrhenius plot, a value of $Q$ of 142 kJ mol$^{-1}$ is obtained, with $R^2$ of 0.999 from the best straight line fit of the three data

points. Assuming a liquidus temperature of 965°C, the highest estimate for $Q$ from the line for $\Delta s_r = 0$ is 199 kJ mol$^{-1}$; for $\Delta s_r = 14$, the predicted $Q$ is 154 kJ mol$^{-1}$.

## V. Discussion

The analysis in Section 4 of our experimental crystal growth data along [100] of devitrite suggest that a lower bound on the estimate for an apparent Arrhenius activation energy for viscous flow is 257 kJ mol$^{-1}$ at the liquidus temperature; as the temperature decreases, this apparent activation energy increases. By contrast, the normal growth model and suitable consideration of the reduced melting entropy, $\Delta s_r$, produce estimates of $Q$, the activation enthalpy for crystal growth of devitrite along [100], of 262 kJ mol$^{-1}$ (our data), 255 kJ mol$^{-1}$ (a reanalysis of Swift's data from [18]), 277 kJ mol$^{-1}$ (a reanalysis of Dietzel and Flörke's data from [22]), 246 kJ mol$^{-1}$ (a reanalysis of Deubener *et al.*'s data from [7]) and 154 kJ mol$^{-1}$ from a reanalysis of Zanotto's data from [6].

Of these five estimates, the one from Zanotto's work is a clear outlier. This estimate is based upon three data points at very large undercoolings relative to the liquidus temperature of the float glass. Were more data points available from his work at higher temperatures closer to the liquidus temperature, it is entirely possible that these three data points would fit any straight line following from a consideration of Eq. (9) less well, but that the estimate for the activation energy would be higher. For this reason, we feel it is reasonable to exclude this data set when attempting to specify a best estimate of $Q$.

The remaining four data sets produce a best estimate of $Q$ of 260 ± 13 kJ mol$^{-1}$ for crystal growth of devitrite along [100]. This value is tantalisingly close to the lower bound estimate of $Q$ of 256 kJ mol$^{-1}$ from considerations of the viscosity of the float glass as a function of temperature at and below the liquidus temperature shown in Fig. 3. Given the earlier analyses of Preston and Swift,[10,11] in which they both obtained good fits for their crystal growth data for devitrite in terms of the product of the amount of below the liquidus temperature and the reciprocal of the experimental viscosity of the glass at the temperature under investigation, multiplied by a suitable constant, it is appropriate to re-examine Eq. (1) and the replacement of

$$a_0 \nu \exp\left(-\frac{Q}{RT}\right) \text{ by } \frac{k_B T}{3\pi a_0^2 \eta}.$$

Under these circumstances, Eq. (1) can be recast in the form

$$\left(\frac{u}{\Sigma}\right) = \frac{k_B T}{3\pi a_0^2 \eta} \tag{14}$$

using Eq. 10. For small values of $\Delta s_r$ , $\Sigma = \Delta s_r\left(\frac{1}{T_r} - 1\right)$ (Eq. (13)) and, under these circumstances, Eq. (1) becomes

$$\left(\frac{u}{\Sigma}\right) = \frac{k_B \Delta s_r T}{3\pi a_0^2 \eta}\left(\frac{1}{T_r} - 1\right) \equiv \frac{k_B \Delta s_r}{3\pi a_0^2 \eta}\left(T_{liq} - T\right) \tag{15}$$

i.e. a form of the equations considered by both Preston and Swift.

To investigate whether Eq. 14 is appropriate for the data in Table 2, it is useful to rearrange Eq. (14) in the form

$$\ln\left(\frac{u}{\Sigma}\right) = \ln\left(\frac{T}{\eta}\right) + \ln\left(\frac{k_B}{3\pi a_0^2}\right) \tag{16}$$

so that (i) a graph of $\ln(u/\Sigma)$ against $\ln(T/\eta)$ should have a gradient of 1, and (ii) it should be possible to determine a suitable value for the jump distance $a_0$ across the range of growth rates and viscosities under consideration.

Graphs of $\ln(u/\Sigma)$ against $\ln(T/\eta)$ are shown in Fig. 10 for values of $\Delta s_r$ of 1, 5, 14 and 50. It is apparent that for $\Delta s_r$ = 14, the 'best fit' gradient of 0.7731 deviates significantly from the expected slope of 1. Furthermore, the four points at the lower growth rates and higher viscosities seem to have a better fit to an even shallower gradient, while the four points at the higher growth rates would seem to have a better fit to a steeper gradient. Changing the value of $\Delta s_r$ retains the features apparent in the graph for the data set for $\Delta s_r$ = 14, with the clear trend that the gradient increases as $\Delta s_r$ decreases. However, even if $\Delta s_r$ = 1, the 'best fit' gradient is 0.902, still less than 1. Estimates for the jump distance at the temperatures at which crystal growth was measured (Table 2) are shown in Table 5. It is apparent that as $T$ increases, the necessary value of $a_0$ increases systematically, rather than varies about an average value.

This analysis would therefore suggest that the temperature dependence of the crystal growth data has a better fit to Eq. (1) in its usual form, rather than Eq. (14), for this multicomponent system in which more than one devitrification product can occur. We have

to agree with Schmelzer[24] that in multicomponent systems such as float glass, there is an effective diffusion coefficient governing the transport of material across the crystal–glass interface which is a combination of the diffusion coefficients of all components. Therefore in such systems, we conclude that viscosity data cannot be used to describe the transport part of the crystal growth, i.e. it is not appropriate to use the Stokes–Einstein relationship.

A further feature of float glass is its measure of fragility, *m*:

$$m = \left.\frac{\mathrm{d}\left(\log_{10}\eta\right)}{d\left(T_g/T\right)}\right|_{T=T_g} \tag{17}$$

where $T_g$ is the glass transition temperature of the glass.[27] For a glass obeying the VFTH equation, this becomes

$$m = \frac{BT_g}{\left(T_g - T_0\right)^2} \tag{18}$$

Using a value of 553.7°C for $T_g$ at which the float glass has a viscosity of $10^{12}$ Pa s given the values of *A*, *B* and $T_0$ that were used to construct Fig. 3, *m* is found to have a value of 39.7. Coupled with a $B/T_0$ value for this glass of 18.3, these two values suggest that float glass is at least a moderately fragile system, as others have also established (e.g. [27], Table 1, data entry for soda lime silica). It is possible to construct an empirical relationship between *u* and η to take account of this fragility, so that *u* scales as $\eta^{-(1.1-0.005m)}$ [Ref. [33]), but even Ediger *et al.*[33] note that for the empirical relationship they constructed, it was necessary for the liquid and crystal compositions to be the same, a criterion which is not met for the growth of devitrite in soda–lime–silica glass.

## VI. Conclusions

An analysis of experimental crystal growth data along the [100] needle direction of devitrite from a number of sources estimates the activation enthalpy, *Q*, for this process to be 260 ± 14 kJ mol$^{-1}$ when analysed in terms of the normal growth model for crystal growth. This activation energy is higher than values previously reported and tantalisingly close to the apparent activation energy for the viscosity of this glass at its liquidus temperature estimated from its chemical composition. However, while it is tempting to analyse the crystal growth data in terms of the viscosity of float glass as a function of temperature using the Stokes–Einstein relation, it must be remembered that more than one devitrification product

can occur in this multicomponent system, in contrast to one of the major criteria used when modelling crystal growth for fragile glass systems in terms of their viscosity–temperature behaviour. Instead, it would seem better to invoke the concept of the $Q$ we have determined here being an effective diffusion coefficient governing the transport of material across the devitrite–glass interface in float glass, and to recognise that this will be different from the effective diffusion coefficient governing the transport of material across the crystal–glass interface for other possible devitrification products in this system, such as cristobalite and wollastonite.

**Acknowledgements**

We would like to thank the Nuffield Foundation, London, U.K. for the award of an Undergraduate Bursary to RPT during the course of this work. We would also like to thank Dr Iris Buisman of the Department of Earth Sciences at the University of Cambridge for the chemical analysis of the float glass used in this work.

## References

[1]G. W. Morey and N. L. Bowen, "Devitrite," *The Glass Industry*, **12** [6] 133 (1931).

[2]M. Ihara, K. Odani, N. Yoshida, J. Fukunaga, M. Setoguchi and T. Higashi, "The Crystal Structure of Devitrite (Disodium Tricalcium Hexasilicate), $Ca_3Na_2Si_6O_{16}$," *Yogyo-Kyokai-Shi*, **92** [7] 373–378 (1984).

[3]V. Kahlenberg, D. Girtler, E. Arroyabe, R. Kaindl and D. M. Többens, "Devitrite ($Na_2Ca_3Si_6O_{16}$)—Structural, Spectroscopic and Computational Investigations on a Crystalline Impurity Phase in Industrial Soda-Lime Glasses," *Miner. Petrol*., **100** [1] 1–9 (2010).

[4]G. W. Morey and N. L. Bowen, "The Ternary System Sodium Metasilicate–Calcium Metasilicate–Silica," *J. Soc. Glass Technology*, **9** [3] 226–264 (1925).

[5]P. Hrma, D. E. Smith, J. Matyáš, J. D. Yeager, J. V. Jones and E. N. Boulos, "Effect of Float Glass Composition on Liquidus Temperature and Devitrification Behaviour, " *Glass Technol.: Eur. J. Glass Sci. Technol. A* **47** [3] 78–90 (2006).

[6]E. D. Zanotto, "Surface Crystallization Kinetics in Soda–Lime–Silica Glasses," *J. Non-Cryst. Solids*, **129** [1–3] 183–190 (1991).

[7]J. Deubener, R. Brückner and H. Hessenkemper, "Nucleation and Crystallization Kinetics on Float Glass Surfaces," *Glastech. Ber.*, **65** [9] 256–266 (1992).

[8]D. Turnbull and M. H. Cohen, "Crystallization Kinetics and Glass Formation"; pp. 38–62 in *Modern Aspects of the Vitreous State,* Edited by J. D. Mackenzie, Butterworth & Co. Ltd., London, 1960.

[9]V. M. Fokin, M. L. F. Nascimento and E. D. Zanotto, "Correlation between Maximum Crystal Growth Rate and Glass Transition Temperature of Silicate Glasses," *J. Non-Cryst. Solids*, **351** [10–11] 789–794 (2005).

[10]E. Preston, "The Crystallisation Relationships of a Soda–Lime–Magnesia–Silica Glass as Used for Drawn Sheet and the Process of Devitrification," *J. Soc. Glass Technology*, **24** [4] 139–158 (1940).

[11]H. R. Swift, "Effect of Magnesia and Alumina on Rate of Crystal Growth in some Soda-Lime-Silica Glasses," *J. Am. Ceram. Soc*., **30** [6] 170–174 (1947).

[12]H. Insley, "The Microscopic Identification of Stones in Glass," *J. Am. Ceram. Soc*., **7** [1] 14–18 (1924).

[13]A. B. Peck, "A New Glass Stone: $Na_2O \cdot 3CaO \cdot 6SiO_2$," *J. Am. Ceram. Soc*., **9** [6] 351–353 (1926).

[14]A. J. Holland and E. Preston, “The Microscopical Examination and Identification of Crystalline Products in Commerical Glasses,” *J. Soc. Glass Technology*, **21** [5] 395–408 (1937).

[15]A. J. Holland and E. Preston, “The Microscopical Examination and Identification of Crystalline Products in Commerical Glasses. Part II,” *J. Soc. Glass Technology*, **22** [2] 82–98 (1938).

[16]K. M. Knowles, B. Li, C. N. F. Ramsey and R. P. Thompson, “Microstructural Characterisation of Devitrite, $Na_2Ca_3Si_6O_{16}$,” *Advanced Materials Research*, **585** 51–55 (2012).

[17]K. M. Knowles and C. N. F. Ramsey, “Type II Twinning in Devitrite, $Na_2Ca_3Si_6O_{16}$,” *Phil. Mag. Lett.*, **92** [1] 38–48 (2012).

[18]H. R. Swift, “Some Experiments on Crystal Growth and Solution in Glasses,” *J. Am. Ceram. Soc.*, **30** [6] 165–169 (1947).

[19]W. A. Deer, R. A. Howie and J. Zussman, An Introduction to the Rock-Forming Minerals, Longman, Harlow, Essex, U.K., 1966, pp. 340–355.

[20]I. Maki, “Unit Cell Data for Devitrite, $Na_2Ca_3Si_6O_{16}$,” *J. Ceram. Assoc. Japan*, **76** [6] 203–204 (1968).

[21]H. D. Keith and F. J. Padden, “A phenomenological theory of spherulitic crystallization,” *J. Appl. Phys.*, **34** [8] **2**409–2421 (1963).

[22]A. Dietzel and O. W. Flörke, “Gleichgewichtszustände in flüssigem Glas,” *Glastech. Ber.*, **28** [11] 423–426 (1955).

[23]G. W. Morey, “The Devitrification of Soda–Lime–Silica Glasses,” *J. Am. Ceram. Soc.*, **13** [10] 683–713 (1930).

[24]J. W. P. Schmelzer, “Crystal Nucleation and Growth in Glass-Forming Melts: Experiment and Theory,” *J. Non-Cryst. Sol.*, **354** [2–9] 269–278 (2008).

[25]M. L. F. Nascimento and E. D. Zanotto, “Does Viscosity Describe the Kinetic Barrier for Crystal Growth from the *Liquidus* to the Glass Transition?,” *J. Chem. Phys.*, **133** [17] art. 174701 (2010).

[26]B. Moğulkoç, K. M. Knowles, H. V. Jansen, H. J. M. ter Brake and M. C. Elwenspoek, “Surface Devitrification and the Growth of Cristobalite in Borofloat® (Borosilicate 8330) Glass,” *J. Am. Ceram. Soc.*, **93** [9] 2713–2719 (2010).

[27]M. L. F. Nascimento and C. Aparicio, “Data Classification with the Vogel–Fulcher–Tammann–Hesse Viscosity equation Using Correspondence Analysis,” *Physica B*, **398** [1] 71–77 (2007).

[28]T. Lakatos, L-G. Johansson and B. Simmingsköld, “Viscosity temperature relations in the glass system $SiO_2$–$Al_2O_3$–$Na_2O$–$K_2O$–CaO–MgO in the composition range of technical glasses,” *Glass Technology*, **13** [3] 88–95 (1972).

[29]A. Fluegel, A. K. Varshneya, D. A. Earl, T. P. Seward and D. Oksoy, “Improved composition-property relations in silicate glasses, Part I: viscosity,” *Ceramic Transactions*, **170** 129–143 (2005).

[30]A. Fluegel, “Glass viscosity calculation based on a global statistical modelling approach,” *Glass Technol.: Eur. J. Glass Sci. Technol. A*, **48** [1] 13–30 (2007).

**[31]**C. Kröger and G. Kreitlow, “Die Lösungs- und Bildungswärmen der Natronkalksilikate,” *Glastech. Ber.*, **29** [10] 393–400 (1956).

[32]W. D. Kingery, H. K. Bowen and D. R. Uhlmann, Introduction to Ceramics, 2nd edition. John Wiley and Sons Ltd., New York, 1976, Ch. 8, p. 357.

[33]M. D. Ediger, P. Harrowell and L. Yu, “Crystal growth kinetics exhibit a fragility-dependent decoupling from viscosity”, *J. Chem. Phys.*, **128** [3] art. 034709 (2008).

## Figure Captions

Fig. 1 A low magnification photograph of devitrite needles nucleated on the surface of a float glass block after a heat treatment of 17 h at 850°C observed in transmitted polarized light with a sensitive tint at 45° to the polarizer and analyzer, which are aligned vertically and horizontally respectively. The needles are in a thin section cut perpendicular to the surface of the glass block. The edge of the sample of float glass is just above the scale marker.

Fig. 2 Examples of small-angle branching seen in fans of devitrite crystals after careful thinning to produce sections of devitrified glass sufficiently thin, so that different fans do not exhibit excessive overlap when observed by transmitted light polarized light microscopy.

Fig. 3 Plot of the Vogel–Fulcher–Tammann–Hesse (VFTH) equation (bold line) for the Fluegel model[30] for all the eight oxide compositions in Table 1 between 680°C and 965°C. The best fit straight line to the VFTH equation is also shown, together with its equation.

Fig. 4 Analysis of the crystal growth data in Table 1 using Eq. (9), with $u$ in m $s^{-1}$ and with $T_{liq}$ as 965°C (1238 K). Assumed values of $\Delta s_r$ for the data are 0 (◇), 5 (□), 14 ( • ) , 50 ( o ) and ∞ ( + ). The equations of the best fit straight lines for each assumed value of $\Delta s_r$ are shown, together with their $R^2$ values, the squares of their linear correlation coefficients.

Fig. 5 A plot of crystal growth rate against temperature for the data in Table 1 compared with Eq. (9) with $Q$ taking a value of 262 kJ $mol^{-1}$, a $\Delta s_r$ of 14, a $T_{liq}$ of 1238 K, and an $A_0$ of $1.8 \times 10^{14}$ μm $h^{-1}$.

Fig. 6 Analysis of the crystal growth data in Fig. 5 of Swift[18] using Eq. (9), with $u$ in m $s^{-1}$ and with $T_{liq}$ as 1006°C (1279 K). Assumed values of $\Delta s_r$ for the data

◇ □

are 0 (  ), 5 (  ), 14 ( • ) , 50 ( o ) and ∞ ( + ). The equations of the best fit straight lines for each assumed value of $\Delta s_r$ are shown, together with their $R^2$ values.

Fig. 7 Analysis of the crystal growth data from curve I in Fig. 4 of Dietzel and Flörke[22] using Eq. (9), with $u$ in m $s^{-1}$ and with $T_{liq}$ as 962°C (1235 K). Assumed values of $\Delta s_r$ for the data are 0 ( ◇ ), 5 ( □ ), 14 ( • ) , 50 ( o ) and ∞ ( + ). The equations of the best fit straight lines for each assumed value of $\Delta s_r$ are shown, together with their $R^2$ values.

Fig. 8 Analysis of the crystal growth data in Fig. 10a of Deubener et al.[7] using Eq. (9), with $u$ in m $s^{-1}$ and with $T_{liq}$ as 930°C (1203 K). Assumed values of $\Delta s_r$ for the data are 0 ( ◇ ), 5 ( □ ), 14 ( • ) , 50 ( o ) and ∞ ( + ). The equations of the best fit straight lines for each assumed value of $\Delta s_r$ are shown, together with their $R^2$ values.

Fig. 9 Analysis of the crystal growth data in Fig. 4 of Zanotto[6] using Eq. (9), with $u$ in m $s^{-1}$ and with $T_{liq}$ as 965°C (1238 K). Assumed values of $\Delta s_r$ for the data are 0 ( ◇ ), 5 ( □ ), 14 ( • ) , 50 ( o ) and ∞ ( + ). The equations of the best fit straight lines for each assumed value of $\Delta s_r$ are shown, together with their $R^2$ values.

Fig. 10 Plots of $\ln(u/\Sigma)$ against $\ln(T/\eta)$ with $u$ in m $s^{-1}$ and $(T/\eta)$ in K $Pa^{-1}$ $s^{-1}$ for various values of $\Delta s_r$: 1 ( ◇ ), 5 ( □ ), 14 ( • ) and 50 ( o ). The equations of the best fit lines for each set of data are also shown.

Table 1. Chemical composition of float glass for the devitrification experiments in wt%.

| Composition | wt% |
|---|---|
| $SiO_2$ | 72.61 ± 0.13 |
| $Na_2O$ | 12.96 ± 0.05 |
| CaO | 8.98 ± 0.12 |
| MgO | 3.93 ± 0.03 |
| $Al_2O_3$ | 1.00 ± 0.01 |
| $K_2O$ | 0.40 ± 0.02 |
| $Fe_2O_3$ | 0.09 ± 0.01 |
| $TiO_2$ | 0.04 ± 0.01 |

Table 2. Crystal growth data for devitrite.

| $T$ (°C) | $u$ (μm $h^{-1}$) |
|---|---|
| 680 | 0.8 |
| 700 | 1.2 |
| 720 | 2.0 |
| 750 | 5.2 |
| 850 | 75 |
| 900 | 215 |
| 925 | 205 |
| 950 | 135 |

Table 3. Crystal growth measurements in μm at 900°C and 925°C

| Time | Temperature | |
|---|---|---|
| (h) | 900°C | 925°C |
| 1 | 185 | 225 |
| 2 | 380 | 425 |
| 4 | 860 | 826 |

Table 4. Constants *A*, *B* and $T_0$ for the Vogel–Fulcher–Tammann–Hesse viscosity equation with η in Pa s for the chemical composition of float glass shown in Table 1 determined using the models of Lakatos *et al*.,[28] Fluegel *et al*.[29] and Fluegel[30] through Excel spreadsheets available at http://glassproperties.com/viscosity. $T_0$ is shown in the form given as the standard output for these spreadsheets, rather than in K. For the '6 oxides' models, the wt% of $Fe_2O_3$ and $TiO_2$ in Table 1 were taken to be zero and the wt% of the remaining six oxides were rescaled to 100 wt%.

| Model | *A* | *B* (K) | $T_0$ (°C) |
|---|---|---|---|
| Lakatos *et al*.[28] (6 oxides) | –2.8452 | 4692.04 | 236.182 |
| Fluegel *et al*.[29] (6 oxides) | –2.7486 | 4557.8 | 241.3 |
| Fluegel[30] (6 oxides) | –2.7209 | 4523.68 | 246.555 |
| Fluegel *et al*.[29] (8 oxides) | –2.7399 | 4547 | 242 |
| Fluegel[30] (8 oxides) | –2.7156 | 4514.54 | 246.949 |

Table 5. Jump distance estimates for the Stokes–Einstein equation for the crystal growth data in Table 2.

| $T$ (°C) | $a_0$ (Å) |
|---|---|
| 680 | 3.5 |
| 700 | 4.9 |
| 720 | 6.1 |
| 750 | 7.4 |
| 850 | 10.1 |
| 900 | 9.9 |
| 925 | 11.5 |
| 950 | 12.2 |

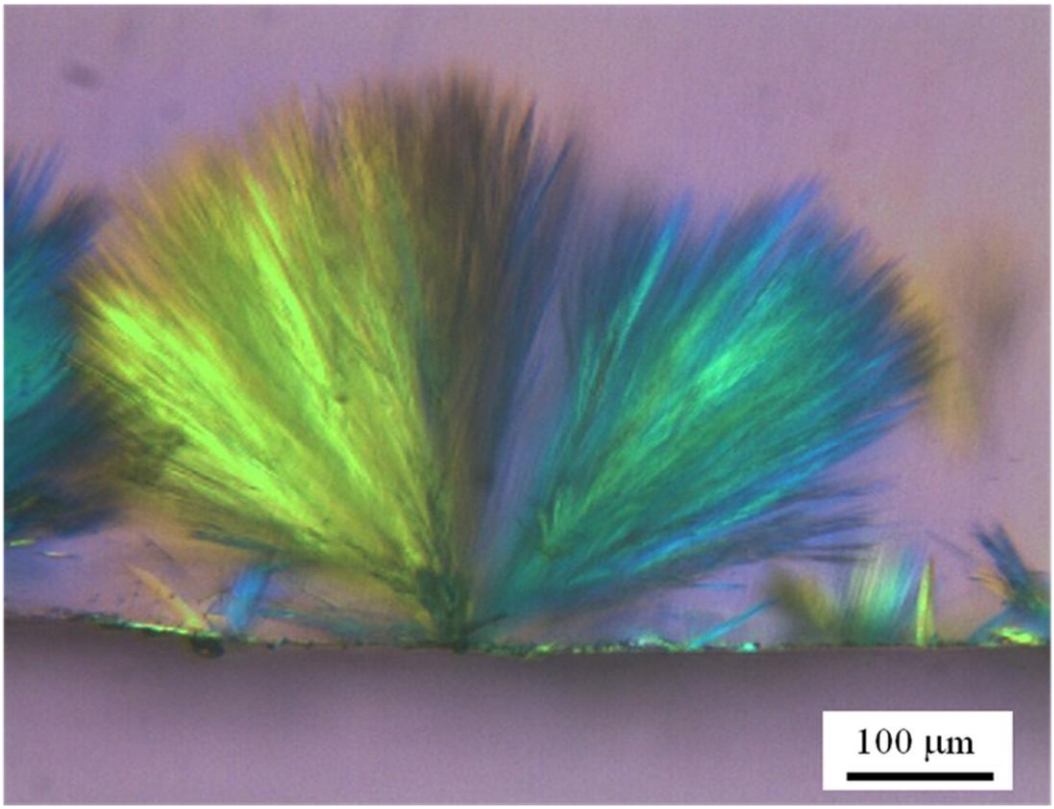


Fig. 1 A low magnification photograph of devitrite needles nucleated on the surface of a float glass block after a heat treatment of 17 h at 850°C observed in transmitted polarized light with a sensitive tint at 45° to the polarizer and analyzer, which are aligned vertically and horizontally respectively. The needles are in a thin section cut perpendicular to the surface of the glass block. The edge of the sample of float glass is just above the scale marker.

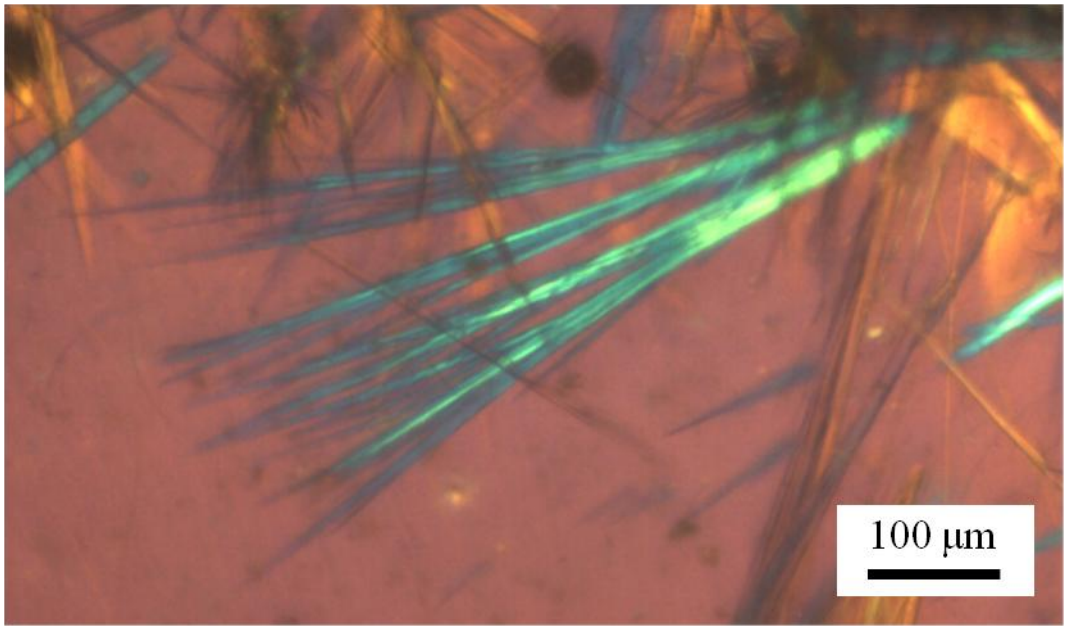


Fig. 2 Examples of small-angle branching seen in fans of devitrite crystals after careful thinning to produce sections of devitrified glass sufficiently thin, so that different fans do not exhibit excessive overlap when observed by transmitted light polarized light microscopy.

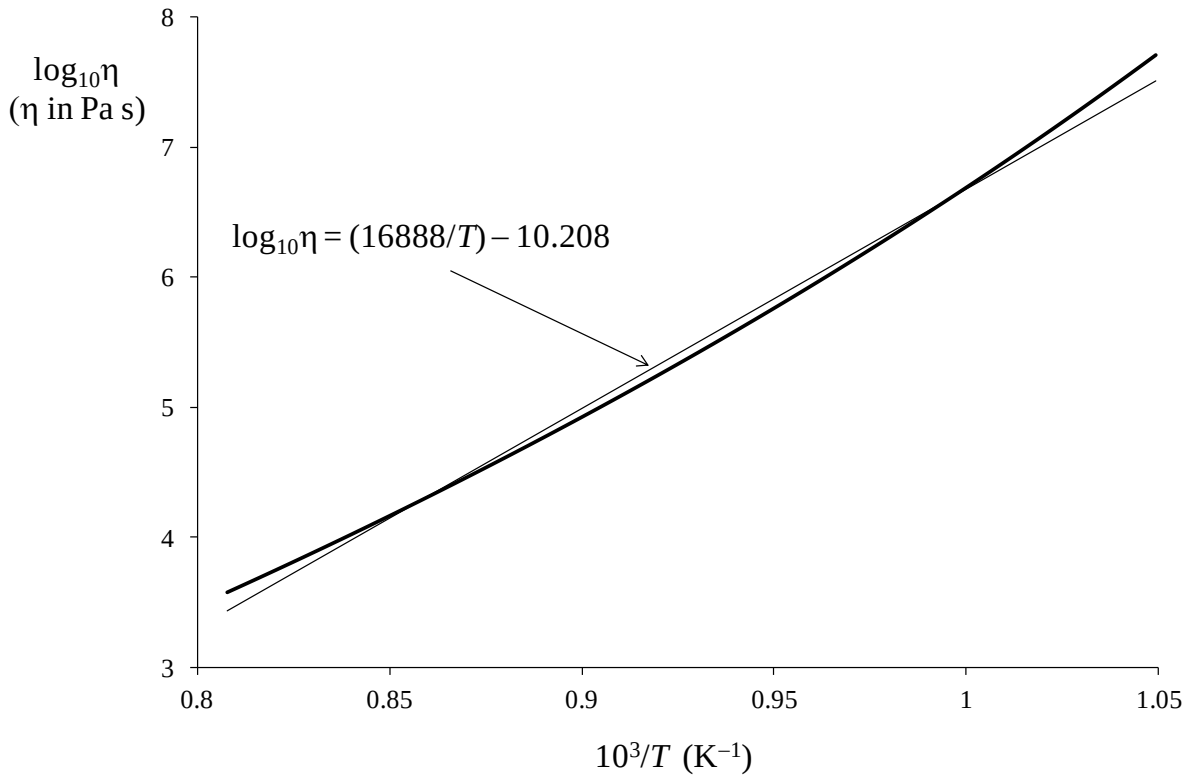


Fig. 3 Plot of the Vogel–Fulcher–Tammann–Hesse (VFTH) equation (bold line) for the Fluegel model[30] for all the eight oxide compositions in Table 1 between 680°C and 965°C. The best fit straight line to the VFTH equation is also shown, together with its equation.

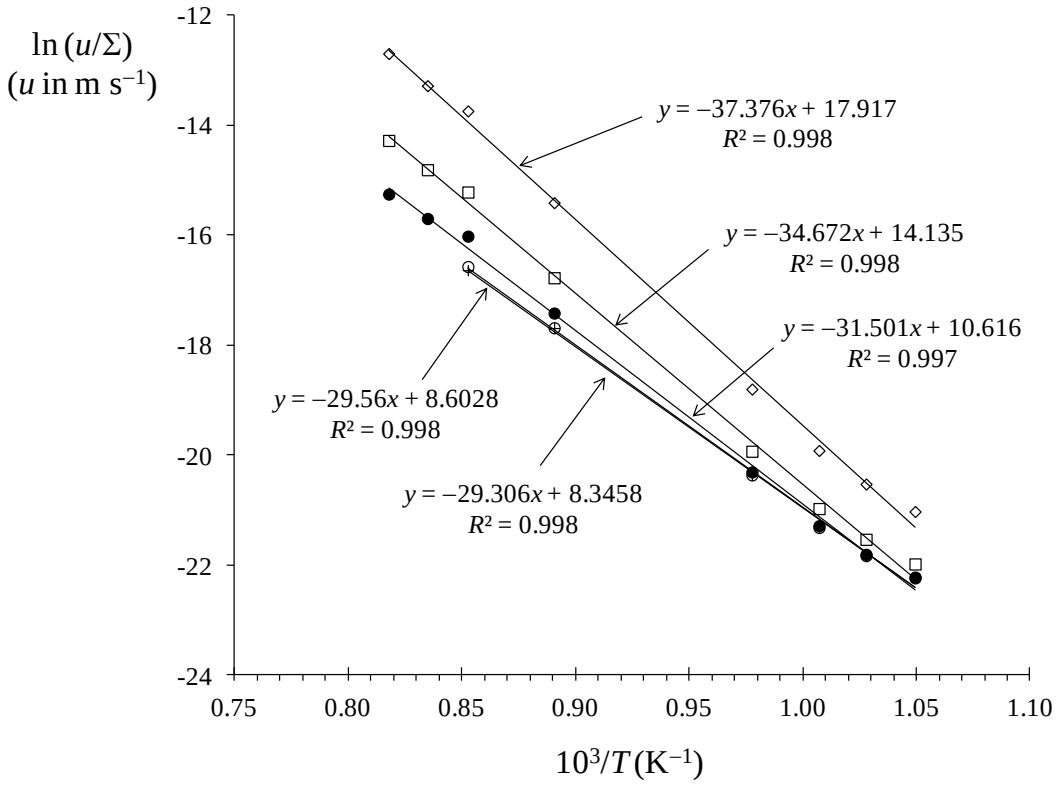


Fig. 4 Analysis of the crystal growth data in Table 1 using Eq. (9), with $u$ in m $s^{-1}$ and with $T_{liq}$ as 965°C (1238 K). Assumed values of $\Delta s_r$ for the data are 0 (◇), 5 (□), 14 ( • ) , 50 ( o ) and ∞ ( + ). The equations of the best fit straight lines for each assumed value of $\Delta s_r$ are shown, together with their $R^2$ values, the squares of their linear correlation coefficients.

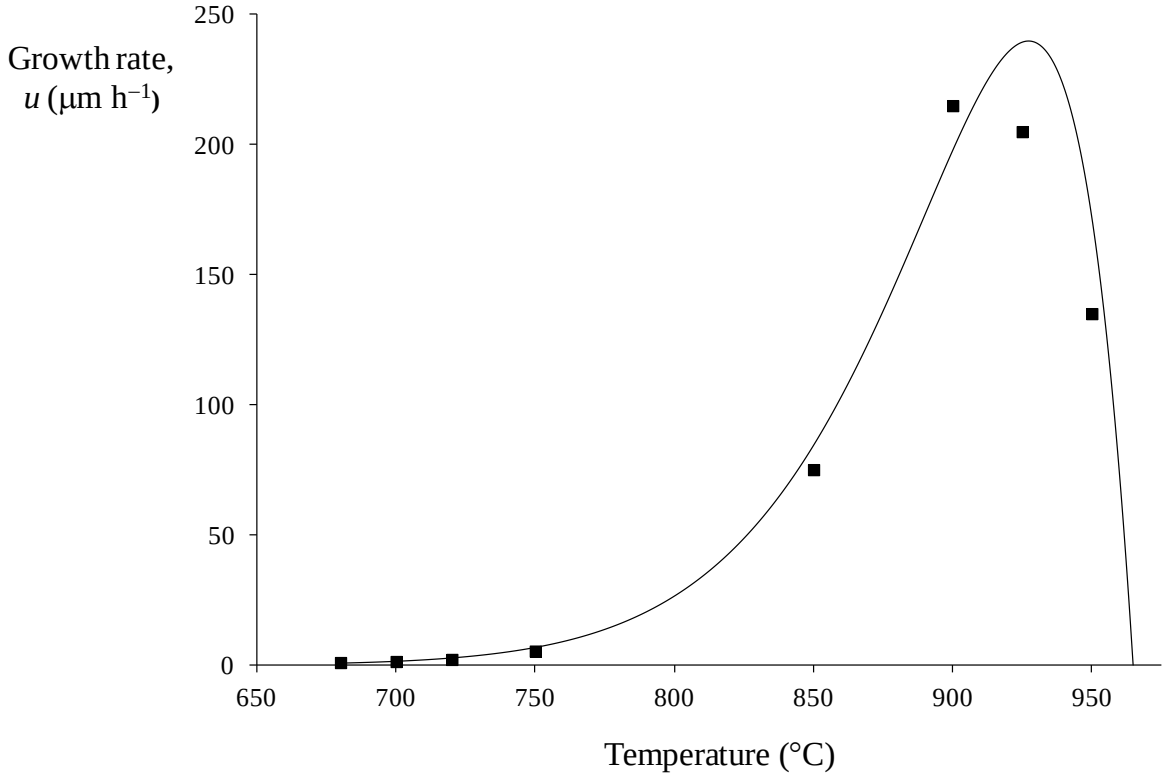


Fig. 5 A plot of crystal growth rate against temperature for the data in Table 1 compared with Eq. (9) with $Q$ taking a value of 262 kJ mol$^{-1}$, a $\Delta s_r$ of 14, a $T_{liq}$ of 1238 K, and an $A_0$ of $1.8 \times 10^{14}$ μm h$^{-1}$.

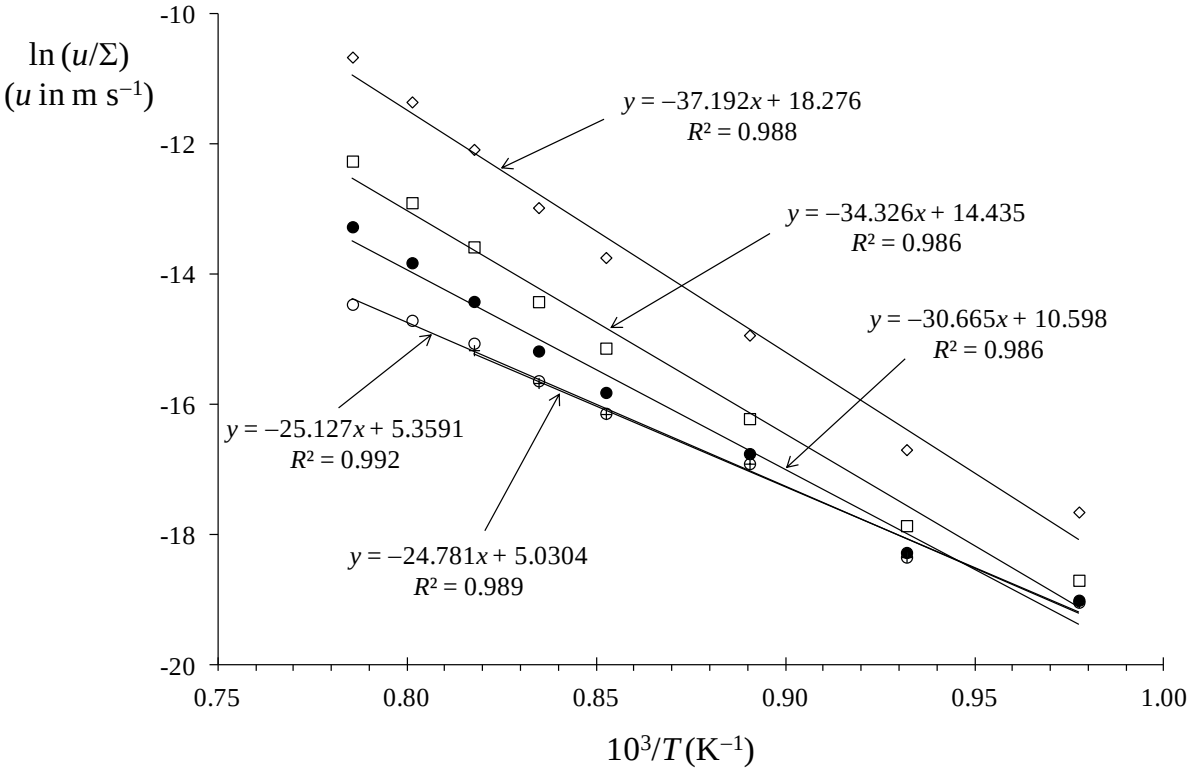


Fig. 6 Analysis of the crystal growth data in Fig. 5 of Swift[18] using Eq. (9), with $u$ in m $s^{-1}$ and with $T_{liq}$ as 1006°C (1279 K). Assumed values of $\Delta s_r$ for the data are 0 ( ◇ ), 5 ( □ ), 14 ( • ) , 50 ( o ) and ∞ ( + ). The equations of the best fit straight lines for each assumed value of $\Delta s_r$ are shown, together with their $R^2$ values.

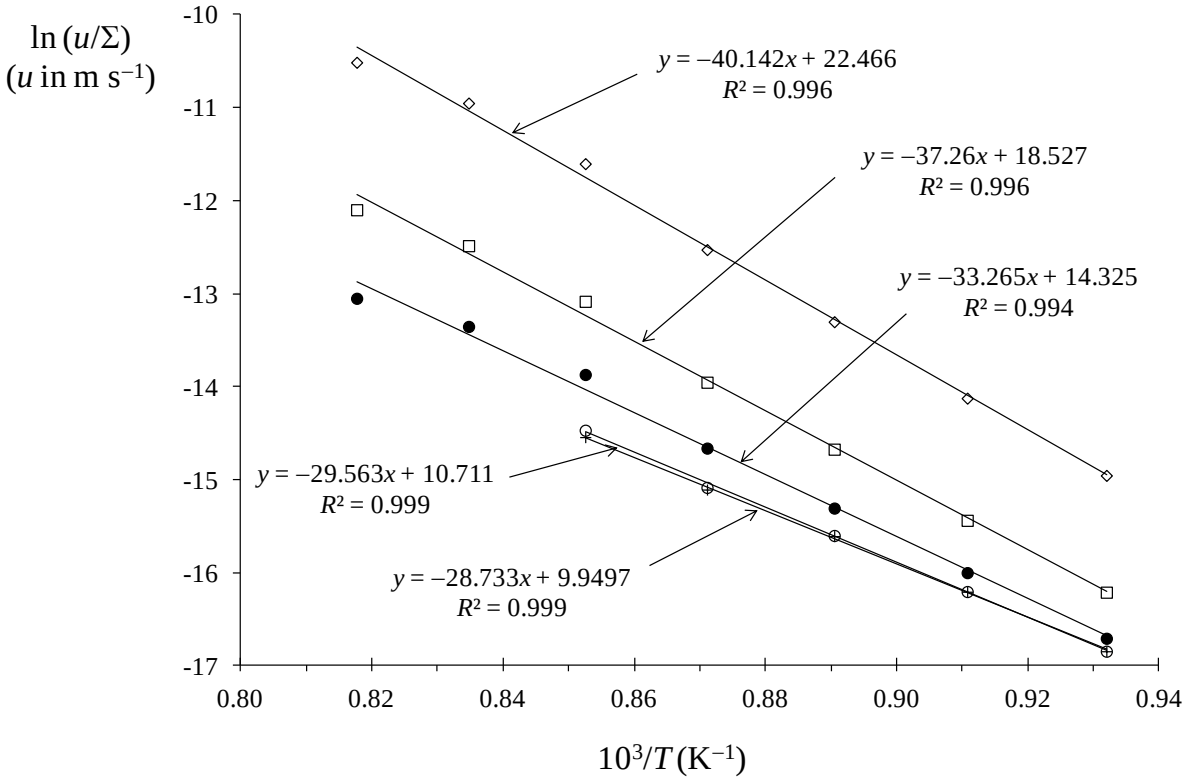


Fig. 7 Analysis of the crystal growth data from curve I in Fig. 4 of Dietzel and Flörke[22] using Eq. (9), with $u$ in m $s^{-1}$ and with $T_{liq}$ as 962°C (1235 K). Assumed values of $\Delta s_r$ for the data are 0 (◇), 5 (□), 14 ( • ) , 50 ( o ) and ∞ ( + ). The equations of the best fit straight lines for each assumed value of $\Delta s_r$ are shown, together with their $R^2$ values.

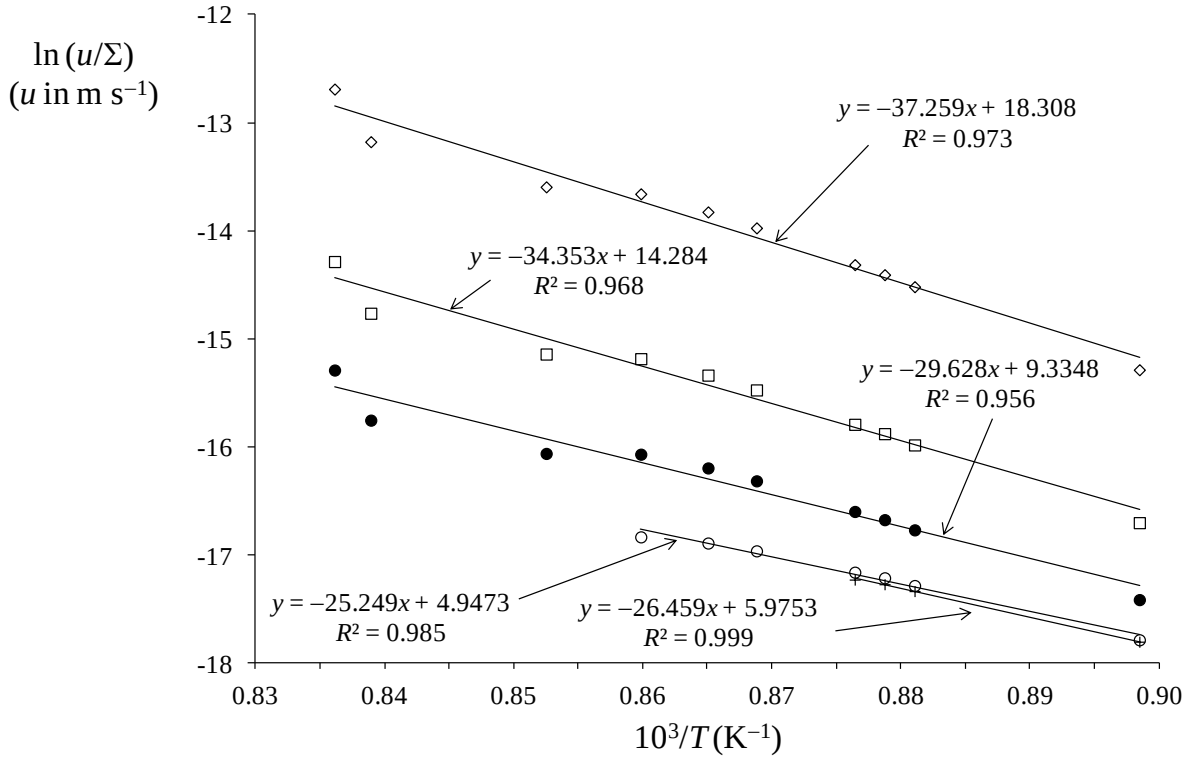


Fig. 8 Analysis of the crystal growth data in Fig. 10a of Deubener et al.[7] using Eq. (9), with $u$ in m s$^{-1}$ and with $T_{liq}$ as 930°C (1203 K). Assumed values of $\Delta s_r$ for the data are 0 ( ◇), 5 ( □), 14 ( • ) , 50 ( o ) and ∞ ( + ). The equations of the best fit straight lines for each assumed value of $\Delta s_r$ are shown, together with their $R^2$ values.

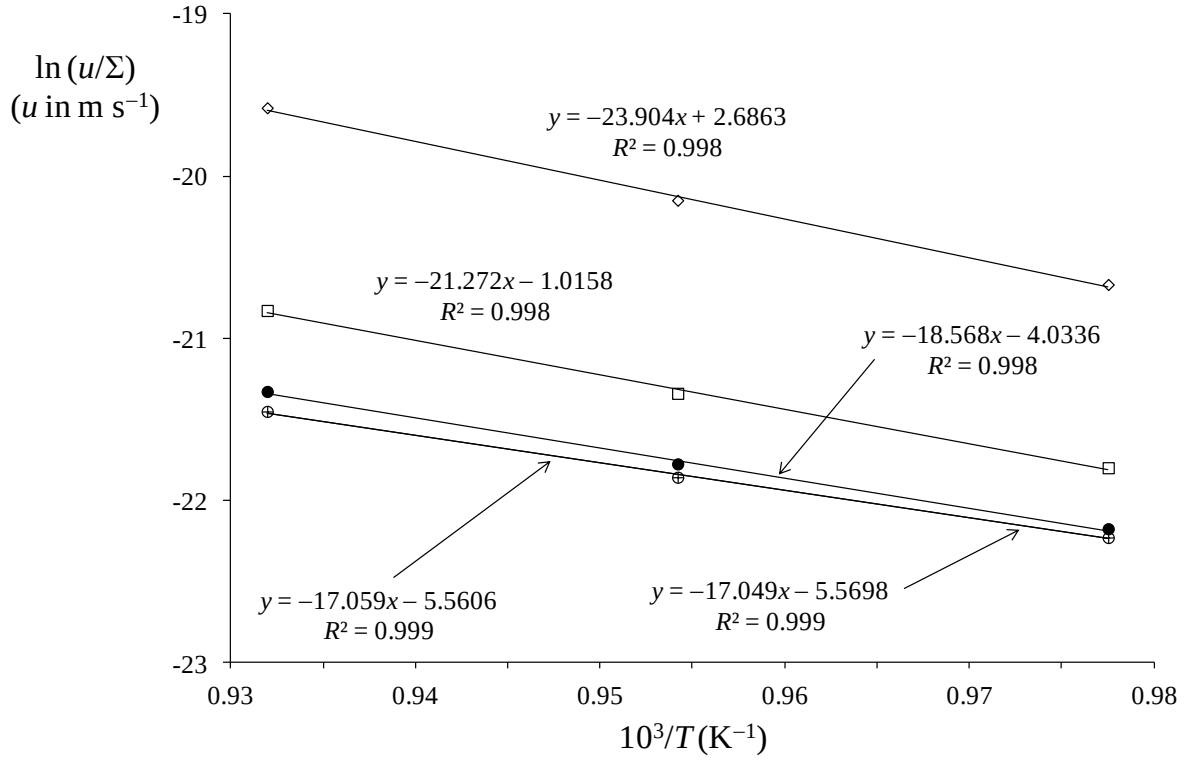


Fig. 9 Analysis of the crystal growth data in Fig. 4 of Zanotto[6] using Eq. (9), with $u$ in m $s^{-1}$ and with $T_{liq}$ as 965°C (1238 K). Assumed values of $\Delta s_r$ for the data are 0 ( ◇ ), 5 ( □ ), 14 ( • ) , 50 ( o ) and ∞ ( + ). The equations of the best fit straight lines for each assumed value of $\Delta s_r$ are shown, together with their $R^2$ values.

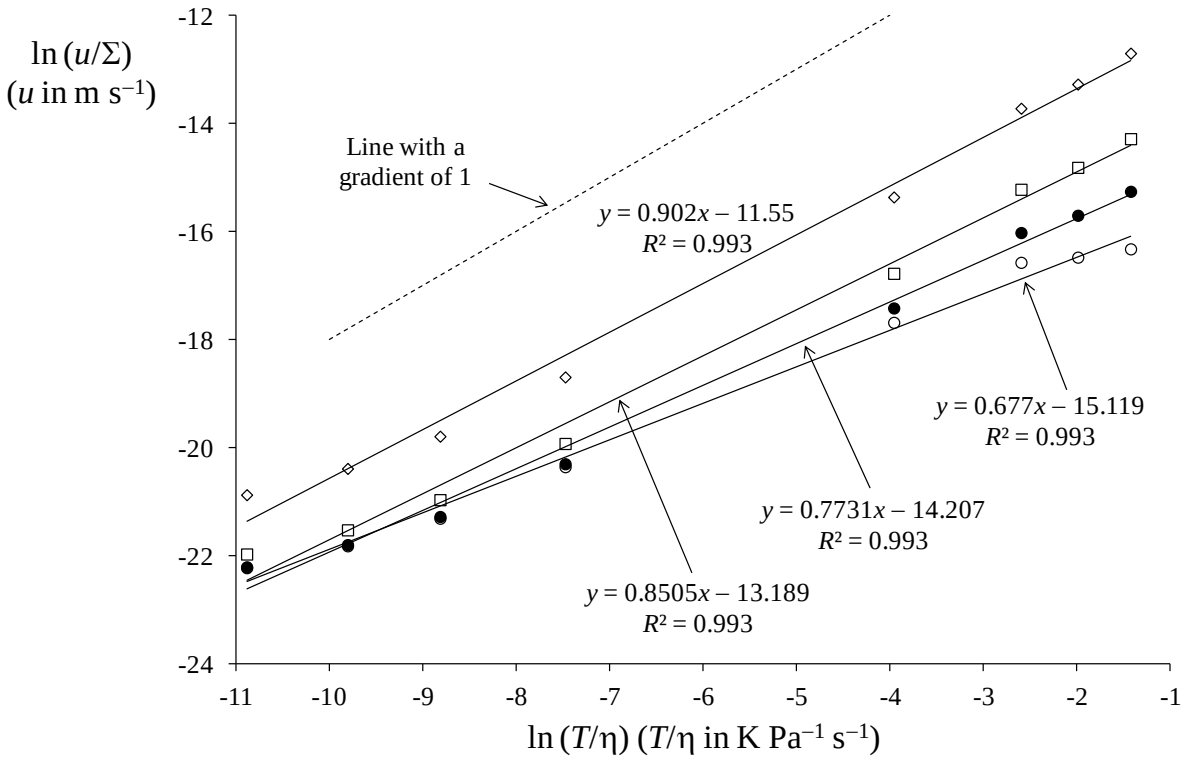


Fig. 10 Plots of $\ln(u/\Sigma)$ against $\ln(T/\eta)$ with $u$ in m $s^{-1}$ and $(T/\eta)$ in K $Pa^{-1}$ $s^{-1}$ for various values of $\Delta s_r$: 1 ( ◇ ), 5 ( □ ), 14 ( • ) and 50 ( o ). The equations of the best fit lines for each set of data are also shown.